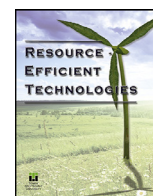


Contents lists available at [ScienceDirect](http://ScienceDirect)

## Resource-Efficient Technologies

journal homepage: [www.elsevier.com/locate/reffit](http://www.elsevier.com/locate/reffit)Green synthesis of silver nanoparticles using *Datura stramonium* leaf extract and assessment of their antibacterial activity<sup>☆</sup>M. Gomathi<sup>a</sup>, P.V. Rajkumar<sup>b,\*</sup>, A. Prakasam<sup>a</sup>, K. Ravichandran<sup>b</sup><sup>a</sup>PG and Research Department of Physics, Thiruvalluvar Government Arts College, Rasipuram, Tamil Nadu 637401, India<sup>b</sup>P.G. & Research Department of Physics, AVVM Sri Pushpam College (Autonomous), Poondi, Thanjavur, Tamil Nadu 613 503, India

## ARTICLE INFO

## Article history:

Received 4 November 2016

Revised 17 December 2016

Accepted 17 December 2016

Available online 11 January 2017

## Keywords:

Green synthesis

Ag NPs

Morphology

Antibacterial

## ABSTRACT

Silver nanoparticles of 15–20 nm size with spherical shape were synthesized from green synthesis method using *Datura stramonium* leaf extract. Synthesized Ag NPs were studied for their optical, structural, surface morphological and antibacterial properties. The optical study shows that the appearance of SPR peak at 444 nm in the absorption spectrum is affirming the formation of Ag NPs and its high intensity with narrowed width indicating the homogenous size and shape of the Ag NPs. Structural studies reveal the good crystalline nature of face center cubic structure of Ag crystal and preferentially oriented along (111) plane with average crystallite size of 18 nm. FTIR analysis exhibits the possible reducing biomolecules within the leaf extract. The well defined homogenous spherical shape of the Ag NPs is clearly observed from the TEM studies and lattice fringes spacing of 0.23 nm shows the high crystalline nature of the synthesized Ag NPs. EDAX profile affirms the Ag crystal by the presence of energy peak at 3 eV. The synthesized Ag NPs showed antibacterial activity against *E. coli* and *S. aureus* bacteria. However, well pronounced activity was observed against *E. coli*.

© 2016 Tomsk Polytechnic University. Published by Elsevier B.V.

This is an open access article under the CC BY-NC-ND license.

<http://creativecommons.org/licenses/by-nc-nd/4.0/>

## 1. Introduction

During the recent decades, vigorous research on metal nanoparticles has been developed speedily because of their excellent optical, electrical, antimicrobial, catalytic, magnetic and other chemical and physical properties; those are entirely different from their bulk counterparts. Silver nanoparticles, one of the most important noble metals, are widely used in photonics [1,2], micro-electronics [3,4], photocatalysis [5,6], and antimicrobial activities [7–10]. Various physical and chemical methods were developed to synthesize metal nanoparticles including electrochemical reduction [11,12], chemical reduction [13,14], heat evaporation [15,16] and microwave irradiation [17,18]. When these methods were adopted to prepare metal nanoparticles, mainly surface passivators are used to prevent the agglomeration of nanoparticles. In the large scale pro-

duction of metal nanoparticles, thiophenol, marcapto acetate and thiourea were applied as passivators having toxic nature which can pollute the environment severely. Moreover, chemical synthesis of nanoparticles may lead to adsorb some toxic chemical species on the surface that can make adverse effects in its applications. Even though there are many means available for metal nanoparticles synthesis, low cost, non-toxic, high-yield and environmental friendly procedures are required to develop metal nanoparticles with desired size and shape thereby biological synthesis process becomes very essential. In biological process, microorganisms like bacteria, actinomycetes and fungi have been studied in metal nanoparticles preparation, while the extract of whole parts of the plants in nanoparticles synthesis appeared as a facile and an alternative to chemical synthesis process.

In this study, we report the synthesis of Ag NPs by green synthesis process using *Datura stramonium* leaf extract as reducing agent. The final products characteristics were studied – optical, structural, surface morphology and elemental analysis. Along with these characteristics, the antibacterial ability against *E. coli* and *S. aureus* was examined and reported.

<sup>☆</sup> Peer review under responsibility of Tomsk Polytechnic University.

\* Corresponding author. Post Graduate &amp; Research Department of Physics, AVVM Sri Pushpam College (Autonomous), Poondi, Thanjavur, Tamil Nadu 613 503, India. Tel.: +918489064520; fax: +91 4374 239328.

E-mail address: [pvrjkumar89@gmail.com](mailto:pvrjkumar89@gmail.com) (P.V. Rajkumar).

## 2. Materials and methods

### 2.1. Preparation of leaf extract and silver nanoparticle (Ag NPs)

*Datura stramonium* leaves were freshly collected from the region of Thanjavur, India. To remove the soil and other contaminants present on the surface of the fresh leaves, initially tap water was used several times to remove the contaminant and then thoroughly washed with de-ionized water. After the wash, 10 g of homogeneous leaves was cut into small pieces and then soaked into 100 mL de-ionized water. These leaves were continuously stirred at 60 °C for 10 min and filtered to get the extract. The extract broth was stored in refrigerator at 4 °C for the further use. 5 mL leaf extract was added drop by drop with 1 mM aqueous solution of silver nitrate ( $\text{AgNO}_3$ ). The reaction mixture of  $\text{AgNO}_3$  and leaf extract was stirred for 2 min to get colloids. The reduction process of  $\text{Ag}^+$  ions to  $\text{Ag}^0$  takes place completely within the period of 5 min and observed visually by varying the initial colour of the reaction mixture from colourless to dark brown. The schematic diagram of preparation of Ag NPs is shown in Fig. 1.

### 2.2. Characterization

The optical absorption spectrum was obtained using UV-vis-NIR spectrophotometer (Perkin Elmer Lambda 35 model) and the X-ray diffraction pattern was recorded using an X-ray diffractometer (PANalytical-PW 340/60 Xpert PRO). Morphology of the sample was observed by transmission electron microscope (TEM, Hitachi H-7100) and elemental analyses were made using energy dispersive X-ray analysis (EDAX). Fourier transform infrared (FTIR) spectrum was measured using Perkin-Elmer RX-I FTIR spectrophotometer.

### 2.3. Assessment of antibacterial activity

Using the well diffusion method, the antibacterial activity of synthesized Ag NPs was tested against Gram positive (*S. aureus*) and Gram negative bacteria (*E. coli*) to find their ability to prevent the bacterial growth. The nutrient agar was poured into the

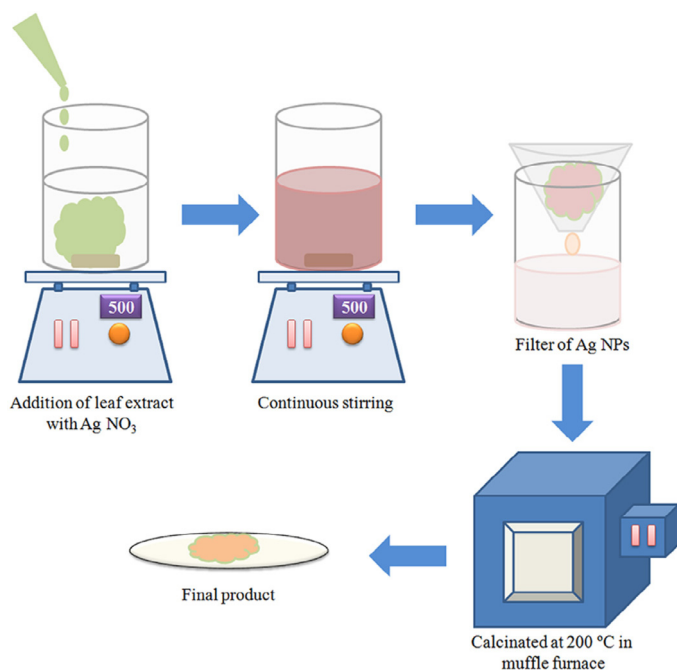


Fig. 1. Schematic diagram of preparation of Ag NPs.

sterilized petriplates and allowed to solidify. After solidification, fresh bacterial culture was spread over the plates by spread plate method. Six wells were made in the agar medium using sterile cork borer; diameter of each well is 5 mm and the well is loaded with different volumes of stock solution such as 50, 100, 150 and 200  $\mu\text{L}$ . For the control and standard antimicrobial agent, stock solution without Ag NPs and streptomycin were used, respectively. The loaded plates were incubated for 24 h at 36 °C. After the incubation, the formation of zone of incubation around the well was observed and scaled in mm; the formed inhibition zone indicates the antibacterial activity of Ag NPs.

## 3. Results and discussion

### 3.1. UV-vis spectroscopy studies

Colloidal dark brown suspension of reaction mixture of  $\text{AgNO}_3$  and leaf extract is a visual and clear evidence of the formation of Ag NPs. This dark brown colour of reaction mixture can be due to resonance of externally applied UV-vis spectrum and collective oscillation caused by the surface electrons of formed Ag NPs; this is well known as Surface Plasmon Resonance (SPR) [19–21]. The initial colour of  $\text{AgNO}_3$  was changed to dark brown with addition of leaf extract after reaction period of 15 min. These colour changes in the reaction mixture strongly indicate the reduction of  $\text{Ag}^+$  ions to  $\text{Ag}^0$ . Due to the formation of Ag crystal in reaction mixture, sharp and narrow SPR peak emerged at 444 nm and is shown in Fig. 2, which may be ascribed to the formation of isotropic spherical Ag NPs [22]. The adequate reducing bio-molecules within the leaf extract greatly reduced the  $\text{AgNO}_3$  solution as silver crystal and wrapped around the Ag NPs.

### 3.2. Structural studies

X-ray diffraction (XRD) pattern of green synthesized Ag NPs was recorded in the  $2\theta$  range 30–80° shown in Fig. 3. The XRD pattern shows the face centre cubic structure of silver crystal, having diffraction peaks at 38, 44.3, 64, 42 and 77.2° correspond to (111), (200), (220) and (311) planes. The diffraction peak at 38° had a robust diffraction intensity indicating the preferential orientation of silver crystal along (111) plane. Non-indexed peak at 46.3° is the diffraction peak related to crystallization of bio-organic phase [23]. The highest peak intensity of (111) plane with narrow FWHM illustrates the good crystalline nature of synthesized Ag NPs as observed from the TEM images. The average crystallite size of Ag NPs

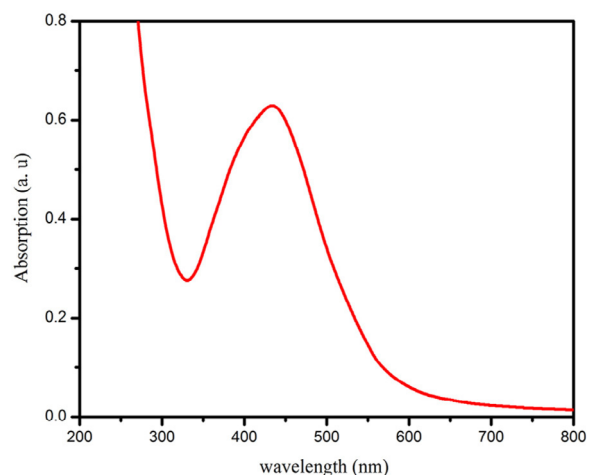


Fig. 2. UV-vis absorption spectrum of Ag NPs.

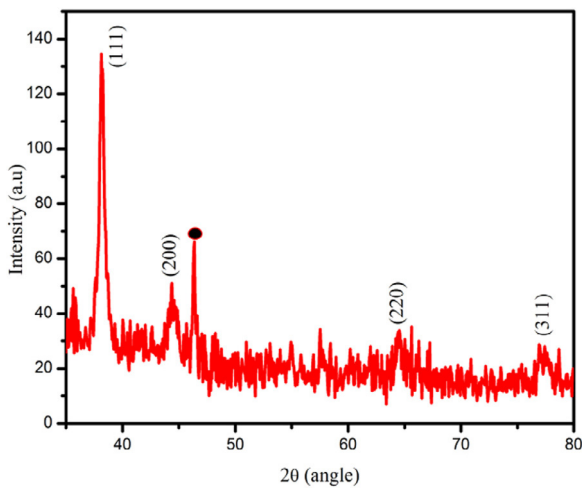


Fig. 3. XRD pattern of Ag NPs.

is calculated from well known Scherrer's formula [24]:

$$D = \frac{0.9\lambda}{\beta \cos \theta}$$

where  $D$  is the crystallite size,  $\lambda$  is the wavelength of X-ray used ( $1.5406 \text{ \AA}$ ),  $\beta$  is the full width at half maximum (FWHM) and  $\theta$  is the Bragg's angle. Synthesized Ag NPs of calculated mean crystallite size was 18 nm.

### 3.3. FTIR analysis

FTIR analysis was studied for synthesized Ag NPs to find out the possible reducing bio-molecules within the *Datura stramonium* leaf extract, and the FTIR spectrum is shown in Fig. 4. The FTIR absorption peaks were observed around 1023, 1110, 1380, 1460, 1517, 1647 and 1738  $\text{cm}^{-1}$ . The absorption peak located at 1023  $\text{cm}^{-1}$  may be owing to  $-\text{C}-\text{O}$  stretching vibrations of alcoholic groups. The peak emerged at 1380  $\text{cm}^{-1}$  is due to  $-\text{C}-\text{O}-\text{C}$  stretching modes. The stretching vibrations at 1110 and 1460  $\text{cm}^{-1}$  are

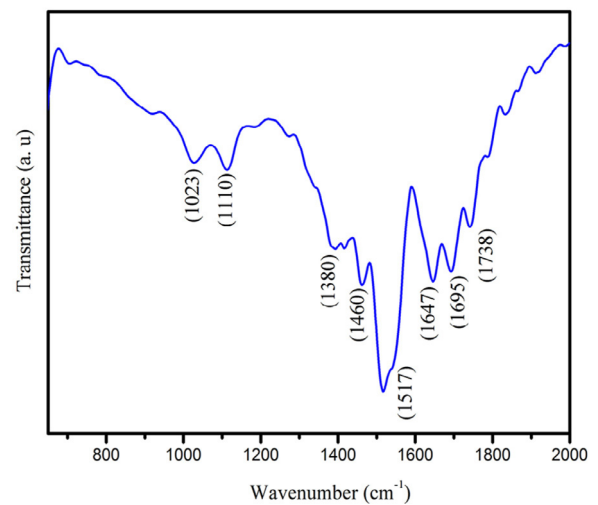


Fig. 4. FTIR spectrum of Ag NPs.

attributed to hydroxyl functional groups in polyphenols and phenols, respectively. The absorption peak at around 1380  $\text{cm}^{-1}$  should be owing to  $\text{C}-\text{N}$  stretching vibration or  $\text{O}-\text{H}$  bending vibrations. The absorption peak at 1738  $\text{cm}^{-1}$  is associated to stretching vibration of  $-\text{C}=\text{O}$  indicating the carboxylic acids group. The presence of stretching vibration at 1641  $\text{cm}^{-1}$  representing that Ag NPs is bounded to proteins via carboxylate group. The stretching vibration of  $-\text{C}-\text{C}-$  in aromatic ring causes an absorption peak at 1571  $\text{cm}^{-1}$ . All these stretching vibrations and bends exhibit that proteins, carboxylic acids, alcoholic groups and polyphenols are bounded along with Ag NPs.

### 3.4. Surface morphological studies and elemental analysis

Fig. 5 (a) shows the TEM image of synthesized Ag NPs. The TEM image affirms that the Ag NPs are in nano scale, maximum of the particles spherical shape in nature with average diameter of 15–20 nm and a few particles are in large scale. These particles

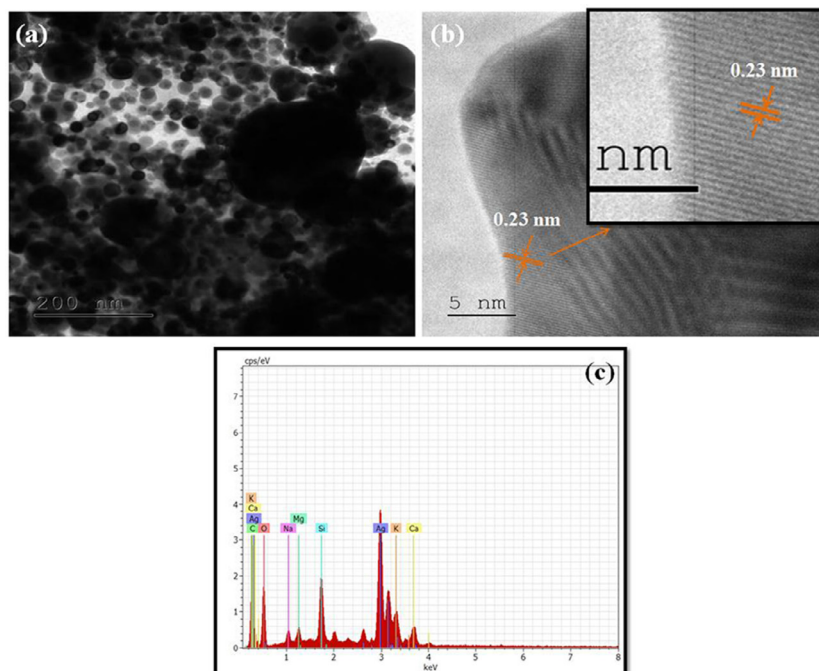


Fig. 5. (a) TEM image, (b) lattice fringes image and (c) EDAX image.

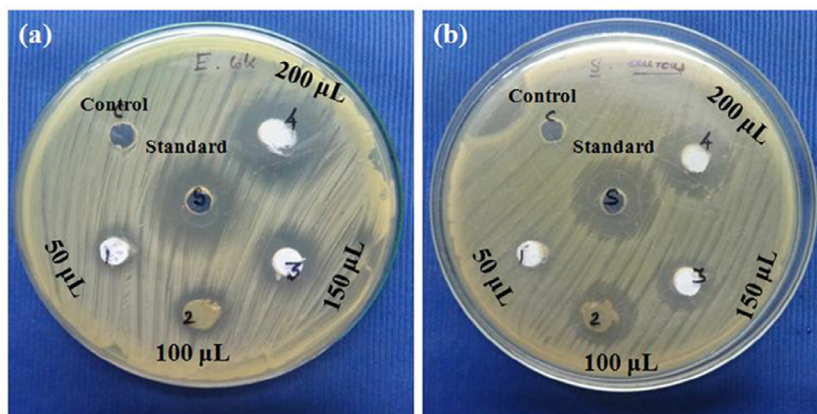


Fig. 6. Antibacterial activity of Ag NPs against (a) *E. coli* and (b) *S. aureus* bacteria.

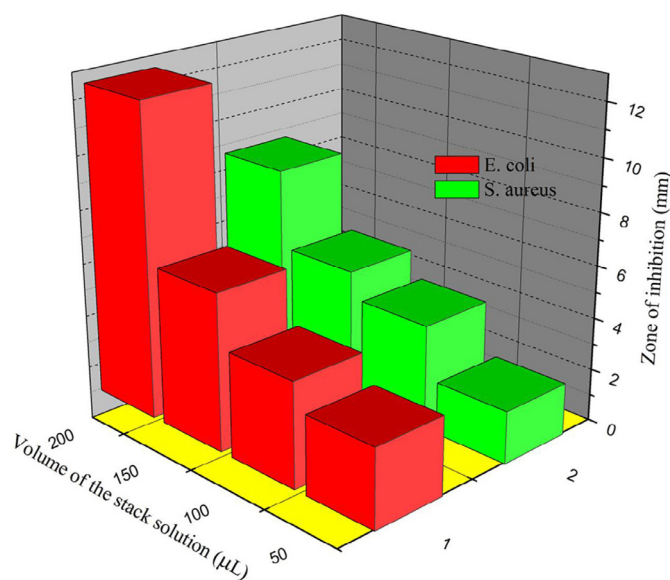


Fig. 7. Variation in zone of inhibition for different stock solution volume against *E. coli* and *S. aureus* bacteria.

are acutely spread over the surface without agglomeration. Highly crystalline nature of the synthesized Ag NPs is clearly identified by the obvious lattice fringes spacing of 0.23 nm in Fig. 5 (b). The EDAX spectrum of Ag NPs is shown in Fig. 5 (c) and exhibits that a strong peak at 3 eV confirms the formation of Ag NPs.

### 3.5. Antibacterial activity

Synthesized Ag NPs were examined about their antibacterial activity against the bacterial strains of *Escherichia coli* (*E. coli*) and *Staphylococcus aureus* (*S. aureus*) using well diffusion technique. The zone of inhibition around the well is shown in Fig. 6. From Fig. 6, it is noted that synthesized Ag NPs show significant impact on the growth of bacteria around the well. No inhibition zone was observed for control, prepared by the stock solution taken in well without Ag NPs. The antibacterial activity of Ag NPs increases gradually as the stock solution increases from 50 to 200 µL. The antibacterial activity of Ag NPs should be associated with several mechanisms including (i) generation of Reactive Oxygen Species (ROS) like super oxide anions ( $O_2^-$ ) and hydroxyl radicals ( $OH^\bullet$ ), (ii) the presence of  $Ag^+$  ions in Ag NPs are making bond with sulphhydryl groups which direct to de-naturation of proteins in the bacteria [25] and (iii) release of  $Ag^+$  ions from the Ag NPs which

simply penetrate into the cell wall and cause severe damage to the bacteria and kill them. Moreover, nanosized Ag NPs were attached to the bacteria and disturb the usual function of bacteria and hence damage severely to outer surface of the bacteria such as DNA, lipids and proteins. From Fig. 6, it is found that Ag NPs have robust antibacterial activity on *E. coli* (Gram negative) than *S. aureus* (Gram positive) bacteria. This greater antibacterial activity against gram negative bacteria is ascribed to the variation in cell wall membrane of these bacteria. The gram negative bacteria such as *E. coli* consist of a very thin layer cell wall membrane, its thickness ranged 7–8 nm and made up of peptidoglycans and lipopolysaccharides [26]. On the other hand, the gram positive *S. aureus* bacteria have a very thick cell wall membrane, its thickness ranged from 20–80 nm and made up of large number of mucopeptides, lipoteichoic and acids murein [27]. In addition, *S. aureus* has an antioxidant enzyme and shows a strong oxidant resistance [28]. Thus, super oxide anions, hydroxyl radicals and released  $Ag^+$  ions can easily penetrate into *E. coli* than *S. aureus* and destroyed the bacteria. The variation in zone of inhibition for different stock solution volume against *E. coli* and *S. aureus* bacteria is shown in Fig. 7.

## 4. Conclusion

Using green synthesis, Ag NPs were synthesized from *Datura stramonium* leaf extract as reducing agent. Optical, structural, surface morphological and antibacterial activities of synthesized sample were examined. From optical study, arising of SPR peak at 444 nm is obviously affirming the formation of Ag NPs in the reaction mixture. XRD profile shows the face centre cubic structure of Ag crystal and the crystallites were preferentially grown along (111) plane with mean size of 18 nm. Possible bio-molecules in the leaf extract to reduce  $Ag^+$  ions to  $Ag^0$  are identified from FTIR spectrum. The spherical shaped Ag NPs with average diameter of 15–20 nm were observed from the TEM image, and the sign of metal Ag is affirming from energy peak at 3 eV. Better antibacterial activity of Ag NPs showed against *E. coli*.

## References

- [1] I.R. Gould, J.R. Lenhard, A.A. Muentner, S.A. Godleski, S. Farid, *J. Am. Chem. Soc.* 122 (2000) 11934–11943.
- [2] J.C. Lin, C.Y. Wang, *Mater. Chem. Phys.* 45 (1996) 136–144.
- [3] G. Schmid, *Chem. Rev.* 92 (1992) 1709–1727.
- [4] W.A. Deheer, *Rev. Mod. Phys.* 65 (1993) 611–676.
- [5] S. Ashokkumar, S. Ravi, S. Velmurugan, *Spectrochim. Acta A Mol. Biomol. Spectrosc.* 115 (2013) 388–392.
- [6] R.J. Chimentao, I. Kirm, F. Medina, X. Rodriguez, Y. Cesteros, P. Salagre, et al., *Chem. Commun.* 7 (2004) 846–847.
- [7] T. Thanh, T. Tran, T.T. Ha Vu, T.H. Nguyen, *Mater. Lett.* 105 (2013) 220–223.
- [8] S. Shankar, J. Chorachoo, L. Jaiswal, S.P. Voravuthikunchai, *Mater. Lett.* 137 (2014) 160–163.

- [9] M. Ghaffari-Moghaddam, R. Hadi-Dabanlou, *J. Ind. and Eng. Chem* 20 (2014) 739–744.
- [10] P.P.N. Vijay Kumar, S.V.N. Pammi, P. Kollu, K.V.V. Satyanarayana, U. Shameem, *Ind. Crops Prod* 52 (2014) 562–566.
- [11] Y.C. Liu, L.H. Lin, *Electrochem. Commun* 6 (2004) 1163–1168.
- [12] G. Sandmann, H. Dietz, W. Plieth, *J. Electroanal. Chem* 491 (2000) 78–86.
- [13] L. Suber, I. Sondi, E. Matijevic, D.V. Goia, *J. Colloid Interface Sci* 288 (2005) 495.
- [14] K. Song, S. Lee, T. Park, B. Lee, *Korean J. Chem. Eng* 26 (2009) 155.
- [15] C.H. Bae, S.H. Nam, S.M. Park, *Appl. Surf. Sci* 197 (2002) 628–634.
- [16] A.B. Smetana, K.J. Klabunde, C.M. Sorensen, *J. Colloid Interf. Sci* 284 (2005) 521–526.
- [17] H. Yin, T. Yamamoto, Y. Wada, S. Yanagida, *Mater. Chem. Phys* 83 (2004) 70.
- [18] M.N. Nadagouda, T.F. Speth, R.S. Varma, *Acc. Chem. Res* 44 (2011) 478.
- [19] M. Ahamed, M.A.M. Khan, M.K.J. Siddiqui, M.S. AlSalhi, S.A. Alrokayan, *Physica E* 43 (2011) 1266–1271.
- [20] C. Krishnaraj, E.G. Jagan, S. Rajasekar, P. Selvakumar, P.T. Kalaichelvan, N. Mohan, *Colloids Surf. B Biointerfaces* 76 (2010) 50–56.
- [21] R.A. de Matos, T. da Silva Cordeiro, R.E. Samad, N.D. Vieira Jr., L.C. Courrol, *Colloids Surf. A* 389 (2011) 134–137.
- [22] V.K. Vidhu, S.A. Aromal, D. Philip, *Spectrochim. Acta Mol. Biomol. Spectrosc* 83 (2011) 392–397.
- [23] K. Mallikarjuna, N.J. Sushma, G. Narasimha, L. Manoj, B.D.P. Raju, *Arab. J. Chem* 7 (2014) 1099–1103.
- [24] P.V. Rajkumar, K. Ravichandran, M. Baneto, C. Ravidhas, B. Sakthivel, N. Dineshbabu, *Mater. Sci. Semicond. Process* 35 (2015) 189–196.
- [25] R.S. Patil, M.R. Kokate, S.S. Kolekar, *Spectrochim. Acta Mol. Biomol. Spectrosc* 91 (2012) 234–238.
- [26] S. Snega, K. Ravichandran, M. Baneto, S. Vijayakumar, *J. Mater. Sci. Technol* 31 (2015) 759–765.
- [27] K. Ravichandran, S. Snega, N. Jabena Begum, K. Swaminathan, B. Sakthivel, L. Rene Christena, et al., *Superlattice. Microst* 69 (2014) 17–28.
- [28] S. Zhao, Y. Zhou, K. Zhao, Z. Liu, P. Han, S. Wang, et al., *Phys. B: Condens. Matter* 373 (2006) 154–156.